



Machine learning-based assessment and simulation of land use modification effects on seasonal and annual land surface temperature variations

Mudassir Khan^a, Muhammad Qasim^b, Adnan Ahmad Tahir^{c,*}, Abida Farooqi^{a,**}

^a Department of Environmental Sciences, Quaid-i-Azam University, Islamabad, Pakistan

^b Department of Environmental and Conservation Sciences, University of Swat, Pakistan

^c Department of Environmental Sciences, COMSATS University Islamabad (CUI), Abbottabad Campus, Abbottabad 22060, Pakistan

ARTICLE INFO

Keywords:

Urbanization
Cellular automata-markov
Artificial neural network
Urban heat island
Machine learning
Urban forest

ABSTRACT

Rapid urban sprawl adversely impacts the local climate and the ecosystem components. Islamabad, one of South Asia's green and environment-friendly capitals, has experienced major Land Use Land Cover (LULC) changes over the past three decades consequently, elevating the seasonal and annual Land Surface Temperature (LST) in planned and unplanned urban areas. The focus of this study was to quantify the fluctuations in LULC and LST in planned and unplanned urban areas using Landsat data and Machine Learning algorithms involving the Support Vector Machine (SVM) over the 1990–2020 data period. Moreover, hybrid Cellular Automata-Markov (CA-Markov) and Artificial Neural Network (ANN) models were employed to project the future changes in LULC and annual LST, respectively, for the years 2035 and 2050. The findings of the study reveal a distinct difference in seasonal and annual LST in planned and unplanned areas. Results showed an increase of ~22 % in the built-up area but vegetation and bare soil decreased by ~10 % and ~12 %, respectively. Built-up land showed a maximum annual mean LST followed by bare-soil and vegetative surfaces. Seasonal analysis showed that summer months experience the highest LST, followed by spring, autumn and winter. Future projections revealed that the built-up areas (~27 % in 2020) are likely to increase to ~37 % and ~50 %, and the areas under the highest annual mean LST class i.e., ≥ 28 °C are likely to increase to ~19 % and ~21 % in planned, and ~38 % and ~42 % in unplanned urban areas for the years 2035 and 2050, respectively. Planned areas have better temperature control with urban green spaces, and controlled infrastructure. The Capital Development Authority of Islamabad may be advised to control the expansion of built-up areas, grow urban forests, and thus mitigate the possible Urban Heat Island (UHI) effect.

1. Introduction

The migration of marginalized communities from underdeveloped to developed areas is one of the major challenges faced by the world community. Within developing countries like Pakistan, every year, people migrate from rural areas to cities for better jobs and

* Corresponding author.

** Corresponding author.

E-mail addresses: mudassirkhan@bs.qau.edu.pk (M. Khan), drqasim@uswat.edu.pk (M. Qasim), Adnantahir@cuiatd.edu.pk (A.A. Tahir), afarooqi@qau.edu.pk (A. Farooqi).

<https://doi.org/10.1016/j.heliyon.2023.e23043>

Received 19 September 2023; Received in revised form 23 November 2023; Accepted 24 November 2023

Available online 29 November 2023

2405-8440/© 2023 The Authors. Published by Elsevier Ltd. This is an open access article under the CC BY-NC-ND license (<http://creativecommons.org/licenses/by-nc-nd/4.0/>).

facilities. This migration results in changing the ecosystem, biodiversity, natural landscapes, topography, and environment of the urban areas [1–5]. Among these topographical changes, deforestation, a decrease in agricultural areas due to the spread of urban areas, and the expansion of barren land are dominant effects of this migration [6]. On the other hand, changes in landscapes also occur due to natural (floods, earthquakes, natural erosion) and anthropogenic activities (urbanization, deforestation, climate change) which have adverse impacts on the surface temperature of the land. However, land use change has both manmade and natural causes. Significant landscape changes have been experienced in recent decades, mainly because of the speedy urbanization that has adverse consequences on the local surface temperature [7].

During the era of unprecedented urban expansion and global climate change, urban land use dynamics and their effects on local and regional climate are significant. The expansion of cities and transformation of urban land surfaces pose a significant threat in the form of UHI and heat strokes for residents. South Asia has recently experienced rapid urbanization. Specifically, Pakistan has become one of the quickest-growing urbanized countries in the world due to the influx of Afghan refugees, population growth, and migration from surrounding areas. The rapid urbanization and population growth have affected the urban climate on a local and regional scale, which replaced green surfaces and soil with grey surfaces which disturbs the energy balance at a local scale. The impervious surface increases the LST [8,9], a widely used parameter in urban thermal research. LST is assessed by the change in energy of the earth's surface and the atmosphere [10]. Therefore, LULC and LST change studies can be used to assess the extent of thermal regime distribution in the context of LULC patterns and anthropogenic activities [11].

Surface temperature is one of the most essential parameters for various environmental studies. For example, ocean circulation, climatic variability, weather prediction, and the energy & water exchange between surface & atmosphere, etc. [12]. LST is affected by the radiation from surface and energy exchange which is stronger during the daytime because of large variations in the response of solar heating between green and impervious surfaces [13]. Modification of vegetative surfaces leads to changes in properties of the land surface which affects the microclimate of the area [14] and increases surface heat. The quantity of solar radiation which is absorbed by the surface and reflected towards the atmosphere is dependent on surface materials. Some materials absorb more energy compared with others because of low reflection, e.g., water and vegetation absorb high energy compared to bare soil, therefore it is cooler than bare soil. The composition, pattern and structure of different LULC classes, as well as properties at pixel level can be significantly influenced by the intensity and variation of urban LST [15,16].

The potential to gain information/data about a phenomenon or a place without physical contact is called remote sensing [17]. Remote Sensing (RS) and GIS give people a deeper understanding of landscape patterns and help to record the energy emitted from the surface and provide historical context of LULC and LST changes [18]. GIS and RS are commonly used for LST and LULC studies [2,11,19]. RS techniques are also widely applied for future LULC and LST simulations. There are several modern methods and algorithms created for LULC modeling purposes. Cellular Automata (CA) [20,21], Markov Chain [22], and Artificial Neural Network (ANN) [23,24] are commonly used for LULC modeling. CA model recognizes the condition of every single cell in the collection according to the earlier condition of the cell in the region as per the already specified conversion guidelines [20]. The CA model is usually used to simulate the future LULC status by utilizing past patterns [25,26].

In the past three decades, Pakistan has experienced significant deforestation and changes in LULC due to anthropogenic and developmental activities. Moreover, there has been a huge influx of people from neighboring districts and cross-border migration from Afghanistan, which has led to changes in LULC and LST in the capital city. These environmental changes in the capital city of Pakistan are not yet studied over a long data period and future projections are not made for better urban planning. It is therefore essential to identify past LULC, seasonal and annual LST patterns and forecast future changes for natural resource management and urban planning

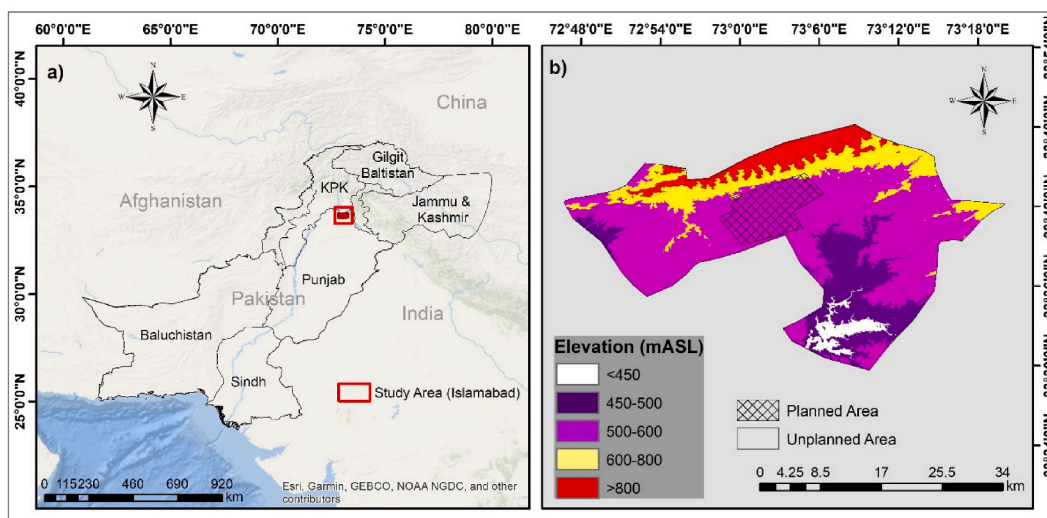


Fig. 1. (a) Location map of Islamabad, and (b) Digital Elevation Model (DEM) of the study area showing different elevation classes, planned and unplanned urban area.

[27]. The main concern of the current study is to evaluate changes in LULC, seasonal and annual LST in past and future scenarios using the CA-Markov model and ANN. The specific objectives of this study are divided into two categories: (i) to analyze changes in LULC, seasonal and annual LST in planned and unplanned urban areas of Islamabad, and (ii) to predict future variations in LULC and annual LST in planned and unplanned urban areas by using the CA-Markov model and ANN in 2035 and 2050.

2. Methodology

2.1. Study area

The study area, Islamabad (capital of Pakistan), is situated between 33° 29' 26.7" – 33° 48' 1.34" North latitude and 72° 48' 42.08" – 73° 22' 48.5" East longitude [Fig. 1 (a, b)]. It is located at the foot of Margalla Mountain at an altitude of 540 m. It is one of South Asia's green and environment-friendly capital. The climate in the study area is a subtropical humid climate (Koppen: Cwa), having four different seasons; (i) winter (December to February), (ii) spring (from March to May), (iii) summer (June to August), and (iv) autumn (September to November). The hottest month in Islamabad is June in which the average temperature remains around 38 °C [28]. With a total population of 2,003,368 (PBS 2017), Islamabad is considered the 9th largest city in Pakistan [29]. Most of the population in the adjacent areas has shifted to the capital city. To provide shelter to these migrated people, a major portion of the land surface has been converted into a settlement area [30] which resulted in rapid urbanization. Expansion of built-up area affected the city's land surface temperature [30].

2.2. Methods

2.2.1. Data sets and pre-treatment process

Landsat satellite imageries were downloaded from TM, ETM+, and OLI sensors for the years 1990, 2005, and 2020, respectively. Satellite remote sensing data was used in the current study to assess the past trend of LULC, and seasonal and annual LST changes. To maximize the classification accuracy, images with a cloud cover of less than 20 % were selected.

Before exporting LULC and LST maps, standard procedures were applied to treat the satellite images. This standard procedure consists of atmospheric correction, radiometric calibration, and gap filling (sensor problem in Landsat 7-ETM+). The treated imageries were then analyzed to detect changes in LULC and seasonal variation in LST by using Google Earth Engine (GEE), ArcGIS, ENVI, and QGIS software.

2.2.2. LULC classification and its accuracy evaluation

LULC classified maps were developed using pre-treated Landsat imageries for the years 1990, 2005, and 2020. All the images were classified into four different classes i.e., built-up, vegetation/green space, barren land, and water-covered areas. In the current study, all the Landsat satellite images were classified by using a supervised classification technique i.e., the Support Vector Machine (SVM) algorithm utilizing GEE and ENVI 5.3 software. Supervised classification is a technique for the quantitative assessment of satellite imagery. It segments the spectral domain of land cover types for LULC classification, which works based on the probability of the assumed training sites. Approximately 50 training samples were drawn for each LULC type to evaluate LULC classification. A confusion matrix with the kappa index was used for measuring the accuracy of the classified images.

2.2.3. Assessment of seasonal and annual LST

Seasonal and annual LST was computed from thermal bands of Landsat images for the years 1990, 2005, and 2020. Band 6 is the thermal band for Landsat 5 and 7 whereas bands 10 and 11 are two thermal bands for Landsat 8. Thermal data obtained by the Landsat satellite is deposited as Digital Numbers (DNs). Following is a four-step process that was used to translate DN to LST.

- **Conversion of Digital Number (DN) into radiation**

Digital Numbers were transformed into radiance using equation (1).

$$L_{\lambda} = \frac{(L_{MINM} + (L_{MAXM} - L_{MINM}) \times DN)}{255} \quad (1)$$

Where L_{λ} is the Spectral Radiance; $L_{MINM} = 1.238$ & $L_{MAXM} = 15.30$ for Landsat 5; $L_{MINM} = 1.238$ & $L_{MAXM} = 15.600$ for Landsat 7; $L_{MINM} = 0.10033$ & $L_{MAXM} = 22.00180$ for Landsat 8 (both band 10 and 11).

- **Conversion of radiance to brightness temperature**

In the second step radiance (from step 1) was converted into brightness temperature (TB) with the help of equation (2).

$$TB = \frac{K2}{\ln((K1/L_{\lambda}) + 1)} \quad (2)$$

Where TB is brightness temperature (in Kelvin); $K1$ & $K2$ are Calibration Constant 1 & 2, having fixed values for Landsat satellite

sensors: ($K1 = 607.76$ & $K2 = 1260.56$ for Landsat 5); ($K1 = 666.09$ & $K2 = 1282.71$ for Landsat 7); ($K1 = 774.89$ & $K2 = 1321.08$ for band 10 of Landsat 8); ($K1 = 480.88$ & $K2 = 1201.14$ for band 11 of Landsat 8).

- **Brightness temperature TB conversion (in Kelvin) into Celsius ($^{\circ}\text{C}$)**

The temperature in Kelvin (brightness temperature) was converted into Degree Celsius ($^{\circ}\text{C}$) by using equation (3).

$$TB (^{\circ}\text{C}) = TB (\text{in Kelvin}) - 273.15 (K) \quad (3)$$

- **Brightness temperature TB conversion ($^{\circ}\text{C}$) into LST**

In the final step, LST was calculated from brightness temperature (TB) using equation (4).

$$LST = \frac{TB}{([1 + (\lambda * TB/\rho) * \ln(\epsilon)])} \quad (4)$$

Where.

λ = Wavelength of emitted-radiation.

$\rho = h * c / s$

$h = 6.626 \times 10^{-34}$ J s (Planck's constant).

$s = 1.38 * 10^{-23}$ J/K (Boltzmann constant).

$c = 2.998 * 10^8$ m/s (Speed of Light).

ϵ is Surface-emissivity

The proportion of vegetation (PV) based on the derivation of NDVI for the years 1990, 2005, and 2020 were used for Surface emissivity. Equation (5) was used to estimate PV.

$$PV = [(NDVI - NDVI_{min}) / (NDVI_{max} - NDVI_{min})]^2 \quad (5)$$

Finally, surface emissivity was calculated using equation (6).

$$\text{Surface emissivity } (\epsilon) = 0.004 * PV + 0.986 \quad (6)$$

LST was calculated from bands 10 and 11 of Landsat 8 therefore an average was taken using cell statistics.

2.2.4. LST standardization

The topographical and climatic variations cause bias; therefore, it is not appropriate to compare variations in seasonal and annual LST for different years without standardization. The calculated seasonal and annual LST was standardized for the years 1990, 2005, and 2020 to make all the changes to be proportional to each other. Standardization was done by using equation (7) [9,31].

$$LST_{\epsilon} = \left(\frac{LST_y - \overline{LST}_{\rho}}{LST_{\delta x}} \right) LST_{\epsilon i} + \overline{LST}_{\alpha} \quad (7)$$

Where;

LST_{ϵ} = normalized LST values for the year y (=1990 or 2020).

LST_y = Original LST values before normalization.

\overline{LST}_{ρ} = average LST values for the year 1990 or 2020.

$LST_{\delta x}$ = standard deviation of LST values for the year 1990 or 2020.

$LST_{\epsilon i}$ = standard deviation of LST values for reference year i (=2005).

\overline{LST}_{α} = average LST value for the year 2005.

2.2.5. Zonal classification of LST

The seasonal and annual LST was classified into 6 classes i.e., $\leq 18^{\circ}\text{C}$, $18^{\circ}\text{C}-20^{\circ}\text{C}$, $20^{\circ}\text{C}-23^{\circ}\text{C}$, $23^{\circ}\text{C}-28^{\circ}\text{C}$ and $\geq 28^{\circ}\text{C}$. This classification was done to evaluate the spatial differences and trends (areal distribution) within different temperature zones in planned and unplanned urban areas of Islamabad.

2.2.6. Simulation of LULC for the future period

For future prediction of LULC changes, different models have been used by previous studies. The choice of the correct simulation technique/model depends on the individual's background (for example, the land reconstruction process, the availability of the data set, the research objectives, and the accuracy of the prediction). In the present study, the CA-Markov model was used for simulation of LULC for 2035 and 2050. A common set of explanatory variables can be created to fully simulate all transitions [32]. First, past changes in land cover (conversion of other land use types to built-up areas) were used as dependent variables; and spatial features (distances between other land use types to settlement areas, water bodies, vegetation, and bare soil) were used as the independent variable.

2.2.7. Simulation of annual mean LST for the future period

LST simulation is based on past data trends. The ANN model was used to analyze a series of previously estimated LST values, understand trends in the data, and predict future changes. Prediction of LST consists of network creation, training of network, network performance-evaluation, simulation, and prediction. Three hidden layers were selected for this study. The selection of hidden layers was made based on multiple trials on the root mean squared error (RMSE) and R^2 values because the network exhibits the non-linear behavior of hidden layers which affect results; therefore, they are imperative to be considered. Normally, the number of hidden layers is kept between the input layer and output layers. A 0.1 learning rate (μ) was put in the initial stage, and decay rate (β) was used for controlling the initial learning. The standard rate of decay ranges from 0 to 1 ($0 < \beta < 1$). A 0.9 decay rate is used to update the learning rate. For example, if the error function between the current and previous iterations is increasing, β upgrades the learning rate μ through division, and multiplies it to reduce μ when the error function decreases. The study conducted by Maduako [33] can be referred to for a detailed description of this method.

3. Results and discussion

3.1. Accuracy assessment and past trends of LULC changes

The overall accuracy in the classification of LULC using the SVM algorithm was 93.03 %, 93.28 %, and 94.03 % for the years 1990, 2005, and 2020, respectively (Table 1). Kappa coefficient was over 0.90 for the entire data period which showed the good accuracy of SVM to classify the different LULC regions.

The past pattern (1990–2020) of the LULC types derived from Landsat satellite imageries is shown in [Fig. 2 (a–c)]. The two trends are distinctive; firstly, the built-up area showed an increasing trend, and secondly, the vegetation and bare soil decreased during the study duration. The results showed modification of vegetation and bare soil into built-up areas. The vegetation and bare soil both decreased by 10.3 % and 11.68 % from 1990 to 2020 (Table 2). The built-up area increased to 22.07 % from 1990 to 2020. Key factors of LULC changes may be related to population growth, economic development, technological development, and some other environmental changes [19]. Among these, population growth is the major factor in LULC change in Pakistan. People are autonomous and equally related to one another for their sustainable development because human beings are the most important natural resource [1].

Islamabad, being the capital of Pakistan is the country's most diverse metropolis in terms of population. It has the largest expatriate and experiences the largest foreigner population in the country [34]. The urban sprawl due to the increase in population in the capital city engulfed a huge quantity of fertile rural land. The same trend of increasing urban areas has been cited in major cities of Pakistan. A 20 % of urban expansion due to urbanization in Lahore is reported by Ref. [35] from 1992 to 2010 and 26.59 % increase in urbanization is analyzed by Ref. [36] in Peshawar from 1999 to 2016 in their studies. Institutional and environmental as well as socio-economic factors may be possible causes of changes in LULC in Islamabad. The findings of this study are in line with that of [37], who argued that economic and geopolitical factors played a key role in increasing urban growth.

3.2. Past patterns of seasonal LST changes in planned and un-planned urban areas

The past pattern of changes in seasonal and annual LST for the years 1990, 2005, and 2020 were derived from Landsat thermal bands [Fig. 3(a–l)] for the unplanned and planned urban areas. The highest mean temperature was recorded 23.27 °C and 23.94 °C (Table 3) in planned and unplanned urban areas, respectively, for summer season in 1990 [Fig. 3(b, f, j)]. The highest annual mean temperature was recorded in unplanned areas of Islamabad i.e., 21.64 °C in 1990.

Annual mean temperature increased by 1.14 °C and 1.91 °C (Table 4) in planned and unplanned areas of Islamabad in 2005. Maximum summer temperature was recorded 34.63 °C and 36.99 °C in planned and unplanned areas, respectively. A 3.76 °C and 2.32 °C increase was found in unplanned and planned areas, respectively, in summer season where maximum temperature was recorded as 36.99 °C and 34.63 °C in unplanned and planned areas, respectively, of Islamabad in 2005.

The highest minimum temperature was noted in summer season and planned urban areas i.e., 27.72 °C [Fig. 3(a–l)] while highest maximum temperature was recorded in unplanned areas i.e., 38.16 °C in 2020 (Table 5). Unplanned urban areas showed the highest annual mean temperature (25.95 °C) as compared to planned areas (23.72 °C) in 2020 [Fig. 4(a–f)].

The high-temperature area (≥ 28 °C) was 0 % in 1990, which increased up to 24.57 % in 2020 (Fig. 5). The area under the temperature range of 23–28 °C increased from 0.10 % (1990) to 73.20 % (2020), and it was converted into a high-temperature zone, while the area under the temperature range of 20–23 °C dropped from 39.39 % (1990) to 2.03 % (2020) (showing a downward trend). These changes may have occurred due to climate change and urbanization. Rapid urbanization (Table 2) characterized by city expansion and climate change may increase the seasonal and annual LST in Islamabad. Rapid urbanization variate thermal conditions of the land by local and regional heating/warming [38]. Therefore, the constant land modifications maximize the warming status of the city. The

Table 1
Accuracy assessment of the classification of LULC for the years 1990, 2005, and 2020.

Year	User Accuracy (%)	Producer Accuracy (%)	Overall Accuracy (%)	Kappa coefficient
1990	94.65	91.96	93.03	0.90
2005	94.78	94.90	93.28	0.91
2020	95.30	93.39	94.03	0.91

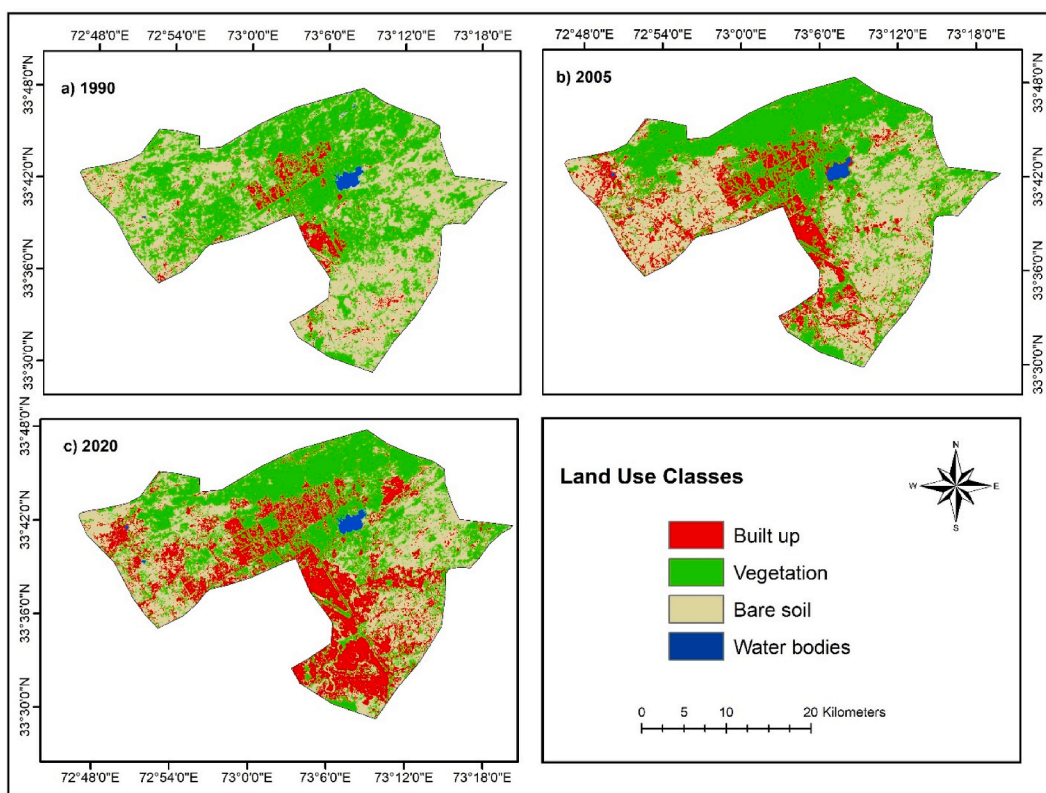


Fig. 2. Land use land cover classified maps of the study area for the years (a) 1990, (b) 2005, and (c) 2020.

Table 2

Net and periodic changes in LULC in Islamabad from 1990 to 2005.

Class name	1990 (km ²)	2005 (km ²)	2020 (km ²)	Change (%)		
				(1990–2005)	(2005–2020)	(1990–2020)
Built up	42.18	135.57	228.70	+11.05	+11.02	+22.07
Vegetation	418.43	340.48	331.42	−9.23	−1.07	−10.3
Bare Soil	377.85	364.45	279.23	−1.59	−10.09	−11.68
Water bodies	6.11	4.76	5.88	−0.16	+0.14	−0.02

average annual temperature in Pakistan has increased by about 0.5 °C over the past 50 years, and the overall precipitation trend is increasing. Likewise, heat wave days per annum have increased approximately by five times compared with 30 years ago [39].

3.3. Variations in temperature in various land cover classes

The temperature in the urbanized areas was found to be the maximum. A decreasing trend was then followed by barren land and vegetation (Fig. 6). The effect of impervious surfaces on LST could be six times higher than that of vegetation and water bodies [40]. The results of the current study is supported by the outcomes of [41], who argued that the LST of the urbanized area and barren land during the day is higher, while the LST of other types (i.e., vegetation and water bodies) is lower. This trend is consistent with [11,37] who studied the relationship between LULC and LST in China's Pearl River Delta and Anger River Sub-basin, western Ethiopia, respectively. The result of the present study showed that the built-up area increased the seasonal and annual LST due to the conversion of vegetation into impervious surface in Islamabad. This means that the warming effect of impervious surfaces is higher than vegetative surfaces. This trend was reported by Ref. [42], which showed a 0.7 °C increase in temperature from 1961 to 2016 and is predicted to be increased by 2.2 °C in 2090. In addition, in this study, it was found that the seasonal and annual LST of all LULC categories increased, even in vegetation (Fig. 6).

This increase in LST over even vegetated areas also indicated the warming effect of urban areas. Ren in 2008 [43] stated the similar urban warming effects in cities and villages of China. Nonetheless, the relatively high rate of temperature rise in Islamabad may be due to the current rapid urban expansion and development. The current study also indicates that there is an urban warming effect in the

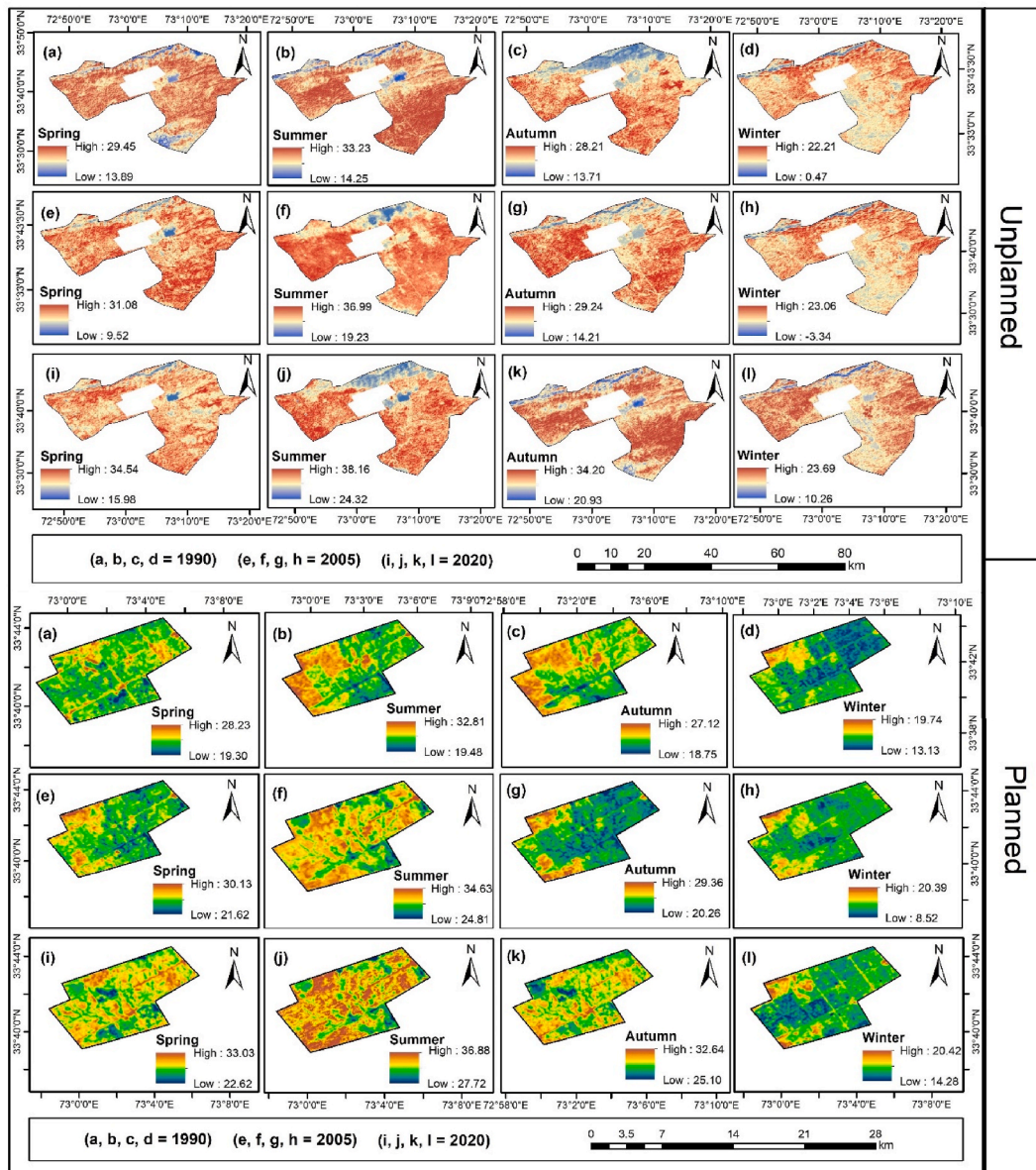


Fig. 3. Seasonal variation in LST (°C) in unplanned and planned areas for the years 1990, 2005, and 2020 in study area. The first, second, third and fourth columns of the figure represent Spring, Summer, Autumn, and Winter, respectively.

Table 3

Seasonal and annual variation in LST (°C) in planned and unplanned urban areas for the year 1990.

Seasons	Planned area				Unplanned area			
	Min	Max	Mean	SD	Min	Max	Mean	SD
Spring	19.30	28.23	22.54	±0.84	13.89	29.45	22.55	±1.32
Summer	19.48	32.31	23.27	±1.07	14.25	33.23	23.94	±1.80
Autumn	18.75	27.12	22.23	±0.96	13.71	28.21	22.01	±1.52
Winter	13.13	19.74	15.10	±0.96	0.47	22.21	15.58	±1.90
Annual	18.19	23.90	20.78	±0.90	12.43	25.29	21.64	±1.42

study area which may result in Urban Heat Island (UHI) as suggested by Ref. [27]. Rapid urbanization sharply decreases urban greenery in unplanned urbanized areas of Islamabad. Vegetation and green surfaces showed a negative relationship with LST [44]. Reduction in green spaces and expansion of impervious surfaces may be the possible reason for increasing LST in Islamabad.

Table 4
Seasonal and annual variation in LST (°C) in planned and unplanned urban areas for the year 2005.

Seasons	Planned area				Unplanned area			
	Min	Max	Mean	SD	Min	Max	Mean	SD
Spring	21.62	30.13	26.55	±1.10	9.52	31.08	26.16	±1.73
Summer	24.21	34.63	29.00	±1.46	19.23	36.99	29.35	±2.00
Autumn	20.26	29.36	22.71	±1.30	14.21	29.24	23.74	±1.80
Winter	8.52	20.39	13.43	±1.30	-3.30	23.06	14.31	±1.90
Annual	20.12	26.86	21.92	±1.00	15.09	28.69	23.55	±1.40

Table 5
Seasonal and annual variation in LST (°C) in planned and unplanned urban areas for the year 2020.

Seasons	Planned area				Unplanned area			
	Min	Max	Mean	SD	Min	Max	Mean	SD
Spring	22.62	33.03	23.86	±0.61	15.98	34.54	23.74	±1.26
Summer	27.72	36.88	32.37	±1.23	24.32	38.16	32.39	±1.80
Autumn	25.10	32.64	28.57	±1.00	20.93	34.20	28.34	±1.70
Winter	14.28	20.42	16.89	±0.86	10.26	23.69	18.13	±1.60
Annual	22.94	28.08	23.72	±0.70	18.15	30.57	25.95	±1.20

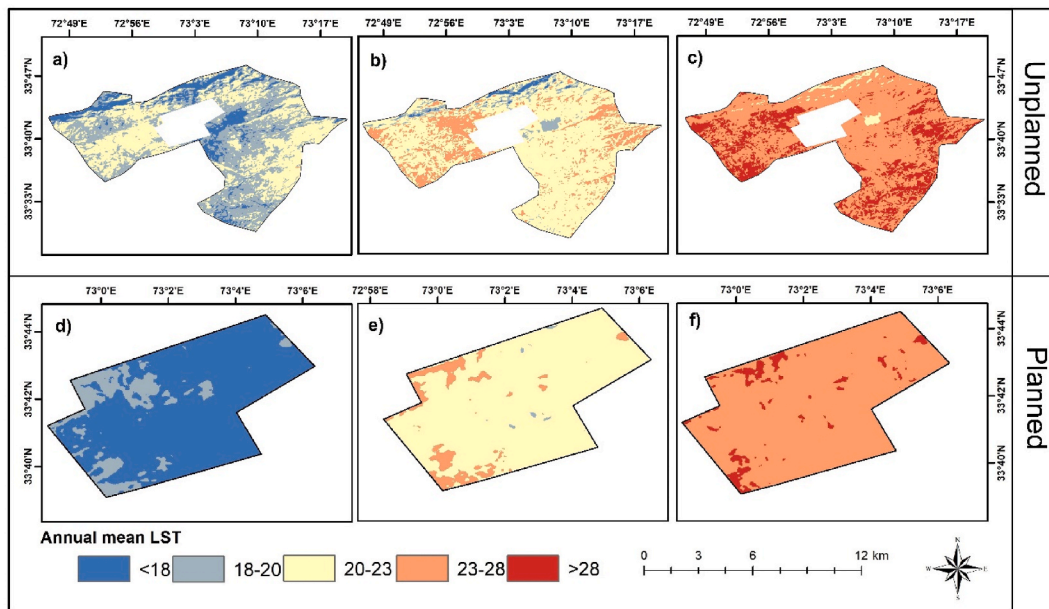


Fig. 4. Variation in annual mean LST (°C) in unplanned and planned areas for the years a,d) 1990, b,e) 2005, and c,f) 2020.

3.4. Simulation of the future land cover dynamics

As the analyzed LULC classes significantly altered during the studied duration (1990–2020) in the area as presented in Table 2 & Figure 2 (a – c)], it is imperative to predict the dynamics of the future land cover through simulation. For this purpose, the CA-Markov model was utilized to predict future LULC for the years 2035 and 2050. As previously mentioned, it uses the past pattern of a cell from a neighborhood and predicts the scenario of each cell as per the standardized transition rules [20]. Therefore, if the LULC change rate is assumed to be constant, the model can reliably predict the future changes of LULC. Approximately, 10.22 % and 12.32 % of the area seem to be converting into built-up areas in 2035 and 2050, respectively (Table 6 & [Fig. 7 (a, b)]). The results showed a good agreement between the future projected results and the classified LULC types for the base period. As indicated by the simulation results, it is expected that the LULC will change in the future, which may adversely impact the environment, changing the climate and biodiversity of the region.

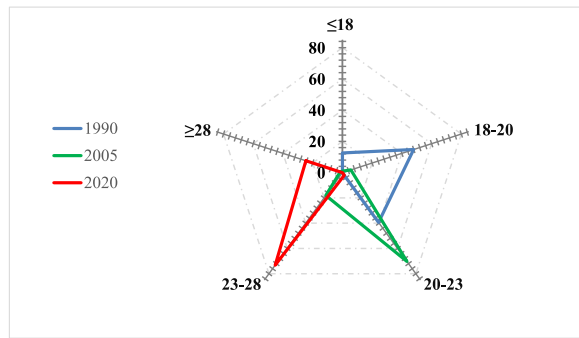


Fig. 5. Area distribution trend (%) in annual mean LST (°C) classes in Islamabad from 1990 to 2020.

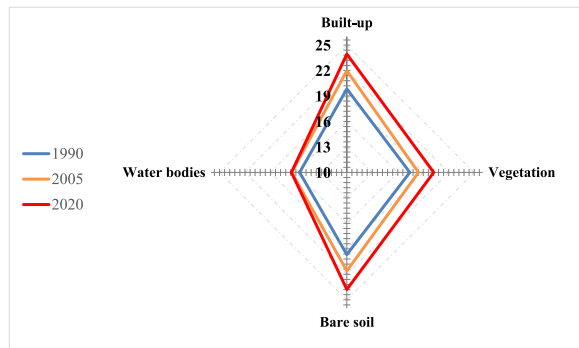


Fig. 6. Fluctuation in annual mean LST (°C) over different LULC classes in Islamabad from 1990 to 2020.

Table 6
Projected changes in LULC for the years 2035 and 2050.

Class name	2035 (%)	2050 (%)
Built up	37.28	49.6
Vegetation	38.41	34.57
Bare soil	23.65	15.18
Water bodies	0.63	0.63

3.5. Planned and unplanned areas of Islamabad under future mean LST

Like the LULC category, annual mean LST during the research data period (1990–2020) also showed significant changes in planned and unplanned urban areas (Fig. 5). Hence the annual mean LST for the future periods (2035 and 2050) is also simulated in planned and unplanned areas of Islamabad [Fig. 8 (a – d)]. The annual mean LST trend estimated based on past data which is used in the ANN model to simulate the future trend in the study area. The results predicted that about 38.66 % and 42.83 % of the unplanned area (Islamabad) falls into the highest temperature class ($\geq 28^\circ\text{C}$) in 2035 and 2050 (Table 7). Planned urban areas showed less variation in temperature as the highest LST class ($\geq 28^\circ\text{C}$) will be 19.75 % and 21.99 % in 2035 and 2050 (Table 7), respectively. Such high temperatures may prove to be dangerous for human health, and animal and plant species.

Therefore, an increase in seasonal and annual LST will also influence the heat capacity of LULC types, leading to the UHI effect, which is caused by the transformation of the ground surface, which is conducive to heat capture and anthropogenic heat release [27, 45]. It will increase the temperature in urban areas instead of in rural areas. An increase in temperature and anthropogenic heat release are among the major environmental concerns for the research since they are detrimental to humans, biodiversity, and the overall ecosystem. Green self-awareness may change individual’s behavior to take part in urban plantation and afforestation drives by the governmental and non-governmental organizations to increase green surfaces which may control the UHI effect [46].

The 5th Assessment Report (AR) of IPCC [47] reported warming in South Asia may exceed the global average and may affect the melting of glaciers and precipitation trends. This will ultimately adversely affect the efficiency of water-dependent sectors such as agriculture and energy. The Sixth AR of IPCC [48] showed the highest land surface temperature of the record.

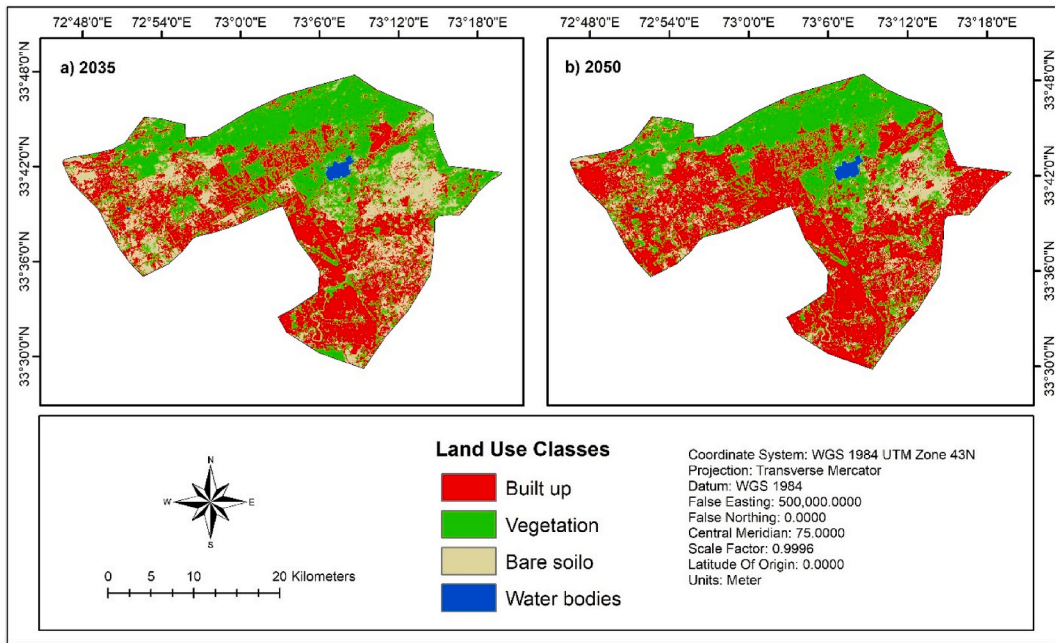


Fig. 7. Simulated land use landcover classified maps of Islamabad for the years (a) 2035, and (b) 2050.

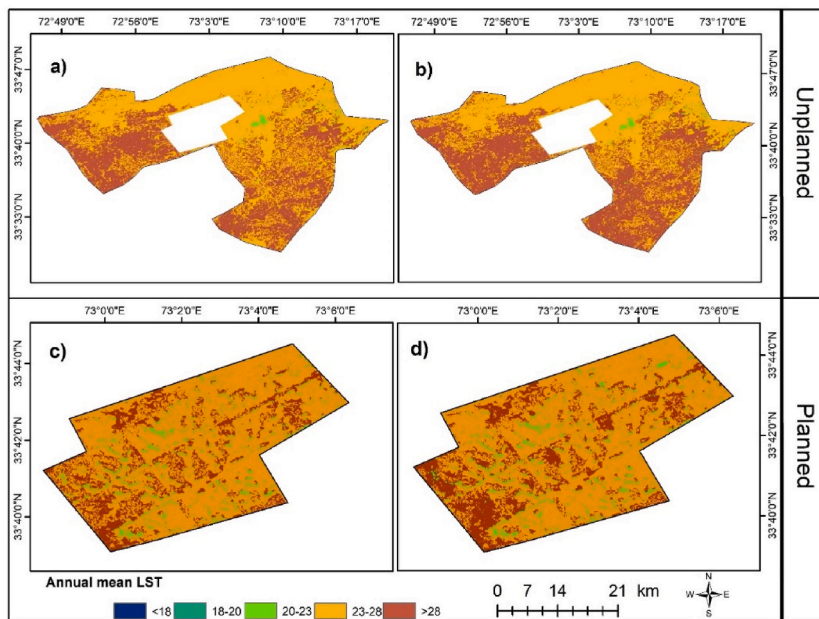


Fig. 8. Projected annual mean LST (°C) map of unplanned and planned areas, Islamabad for the years a,c) 2035, and b,d) 2050.

3.6. Practical implications and limitations

Satellite-based observations of variations in LULC and LST play a crucial role in urban planning and management. According to the current study, there are more green spaces in planned urban areas as compared to unplanned urban areas. These green spaces contribute to regulate seasonal and annual temperature. The transition between green and impervious surfaces and its effect on land surface temperature in unplanned areas were maximum. Planned cities with sufficient green spaces regulate the city’s temperature. The findings of the current study may be fruitful for urban planners and managers to design cities with sufficient green spaces to better control the effect and severity of UHI. It may help scientists, urban planners, and policy makers to identify the rate of urbanization,

Table 7

Projected area (unplanned and planned) of Islamabad under various mean LST classes for the years 2035 and 2050.

LST Class (°C)	Unplanned area (%)		Planned area (%)	
	2035	2050	2035	2050
<18	0.00	0.00	0.00	0.00
18 to 20	0.00	0.00	0.00	0.00
20 to 23	4.94	3.67	1.93	2.03
23 to 28	59.41	55.14	75.31	72.84
≥28	38.66	42.83	19.75	21.99

transition between green and impervious surfaces, UHI creation and its effect on local and regional climate.

However, there are some limitations that exist in the current study. The first limitation is the resolution of Landsat satellite i.e., spatial resolution of 30 m × 30 m and temporal resolution of 16 days, which makes it impossible to calculate micro-level LST variations on a daily basis. Meteorological conditions like rainfall, wind speed, and soil moisture might contribute to variations in LST. These meteorological conditions were not studied due to lack of ground-based sensors and observations. More reliable and precise analysis could be done with finer resolution satellite data along with ground-based sensors and thermal detector.

4. Conclusions

The current study focused to analyze and predict the changes in LULC and LST in planned and unplanned urban areas in the capital city of Pakistan. Support Vector Machine (SVM) algorithm was used for LULC classification of the study area. Seasonal and annual mean LST was derived from the information stored in Landsat's thermal bands. Changes in LULC and annual mean LST were simulated for 2035 and 2050 using a hybrid CA-Markov and an ANN model, respectively. This study concluded that significant changes were evident in LULC during the study duration. Specifically, built-up land increased by ~22 %, while vegetation and bare soil decreased by ~10 % and ~12 %, respectively, from 1990 to 2020. Built-up land showed the highest annual mean LST (23.94 °C) which is followed by bare soil (23.78 °C), green surfaces (20.23 °C), and water bodies in the year 2020. The future prediction results indicated that the built-up area will be increased to 37.28 % and 49.60 % in 2035 and 2050, respectively. Similarly, the areas associated with the annual mean LST class (≥28 °C) are likely to be increased to 38.66 % and 42.83 % in unplanned urban areas and 19.75 % and 21.99 % in planned urban areas in 2035 and 2050, respectively. The findings of this study are a challenge for urban planners to control the unplanned urban growth in the study area. The method proposed by Ref. [27] can be applied to our study area to control the UHI effect and to create a better urban environment. Furthermore, the urban plantation in the centers of the city is the best possible solution to mitigate the UHI formation.

Data availability statement

Data will be made available on request.

Additional information

No additional information is available for this paper.

CRediT authorship contribution statement

Mudassir Khan: Writing - original draft, Visualization, Validation, Investigation, Formal analysis, Data curation, Conceptualization. **Muhammad Qasim:** Writing - review & editing, Software, Resources, Investigation. **Adnan Ahmad Tahir:** Writing - review & editing, Supervision, Project administration, Methodology, Conceptualization. **Abida Farooqi:** Writing - review & editing, Supervision, Project administration, Investigation, Formal analysis, Data curation.

Declaration of competing interest

The authors declare the following financial interests/personal relationships which may be considered as potential competing interests: Associate Editor in "Earth Science Section" of Heliyon - A.A.T. If there are other authors, they declare that they have no known competing financial interests or personal relationships that could have appeared to influence the work reported in this paper.

References

- [1] J.M. Abdula, Land Use/Land Cover Changes, Driving Forces and Their Implications on Climate Variability: the Case of Kereba Sub-catchment of Awash Basin, Eastern Ethiopia, academia, edu, 2021.
- [2] M. Majid, Land use change optimization using a new ensemble model in Ramian County, Iran, Environ. Earth Sci. 80 (23) (2021).
- [3] A. Al Rakib, K.S. Akter, M.N. Rahman, S. Arpi, A.-A. Kafy, Analyzing the pattern of land use land cover change and its impact on land surface temperature: a remote sensing approach in Mymensingh, Bangladesh, Student Res. Conf (2020).

- [4] K. Hokao, V. Phonekeo, M. Srivanit, Assessing the impact of urbanization on urban thermal environment: a case study of Bangkok Metropolitan, *Int. J. Appl. Sci. Technol.* 2 (7) (2012).
- [5] A.-A. Kafy, N.N. Dey, A. Al Rakib, Z.A. Rahaman, N.R. Nasher, A. Bhatt, Modeling the relationship between land use/land cover and land surface temperature in Dhaka, Bangladesh using CA-ANN algorithm, *Environmental Challenges* 4 (2021), 100190.
- [6] K.S. Kumar, P.U. Bhaskar, K. Padmakumari, Estimation of land surface temperature to study urban heat island effect using Landsat ETM+ image, *International Journal of Engineering Science Technology* 4 (2) (2012) 771–778.
- [7] A.-A. Kafy, et al., Predicting changes in land use/land cover and seasonal land surface temperature using multi-temporal landsat images in the northwest region of Bangladesh, *Heliyon* 7 (7) (2021).
- [8] N. Das, P. Mondal, S. Sutradhar, R. Ghosh, Assessment of variation of land use/land cover and its impact on land surface temperature of Asansol subdivision, *The Egyptian Journal of Remote Sensing Space Science* 24 (1) (2021) 131–149.
- [9] M. Khan, et al., Trends and projections of land use land cover and land surface temperature using an integrated weighted evidence-cellular automata (WE-CA) model, *Environ. Monit. Assess.* 194 (2) (2022) 120.
- [10] J.A. Voogt, T.R. Oke, Thermal remote sensing of urban climates, *Rem. Sens. Environ.* 86 (3) (2003) 370–384.
- [11] M.B. Moisa, I.N. Dejene, B.B. Merga, D.O. Gameda, Impacts of land use/land cover dynamics on land surface temperature using geospatial techniques in Anger River Sub-basin, Western Ethiopia, *Environ. Earth Sci.* 81 (3) (2022) 99.
- [12] E. Valor, V. Caselles, "Mapping land surface emissivity from NDVI: application to European, African, and South American areas," *Rem. Sens. Environ.* 57 (3) (1996) 167–184.
- [13] M. Roth, "Urban heat islands", in: *Handbook of Environmental Fluid Dynamics*, volume two: CRC Press, 2012, pp. 162–181.
- [14] J. Rost, H. Mayer, Comparative analysis of albedo and surface energy balance of a grassland site and an adjacent Scots pine forest, *Clim. Res.* 30 (3) (2006) 227–237.
- [15] Y. Chen, M. Amani-Beni, C. Chen, Y. Liang, J. Li, L. Yang, Projection of urban land surface temperature: an inter-and intra-annual modeling approach, *Urban Clim.* 51 (2023), 101637.
- [16] A. Asgarian, B.J. Amiri, Y. Sakieh, Assessing the effect of green cover spatial patterns on urban land surface temperature using landscape metrics approach, *Urban Ecosyst.* 18 (2015) 209–222.
- [17] J. Wright, T.M. Lillesand, R.W. Kiefer, Remote sensing and image interpretation, *Geogr. J.* 146 (3) (1980) 448.
- [18] T.R. Loveland, R.S. Defries, *Observing and Monitoring Land Use and Land Cover Change*, vol. 153, Washington DC American Geophysical Union Geophysical Monograph Series, 2004, pp. 231–246.
- [19] Y. Yang, X. Yang, E. Li, W. Huang, Transitions in land use and cover and their dynamic mechanisms in the Haihe River Basin, China, *Environ. Earth Sci.* 80 (2021) 1–14.
- [20] I. Santé, A.M. García, D. Miranda, R. Crecente, Cellular automata models for the simulation of real-world urban processes: a review and analysis, *Landsc. Urban Plann.* 96 (2) (2010) 108–122.
- [21] H. Zenil, Compression-based Investigation of the Dynamical Properties of Cellular Automata and Other Systems, 2009 *arxiv.org*.
- [22] H. Baltzer, Markov chain models for vegetation dynamics, *Ecol. Model.* 126 (2–3) (2000) 139–154.
- [23] D.L. Civco, Artificial neural networks for land-cover classification and mapping, *Int. J. Geogr. Inf. Sci.* 7 (2) (1993) 173–186.
- [24] S. Ullah, et al., Remote sensing-based quantification of the relationships between land use land cover changes and surface temperature over the Lower Himalayan Region, *Sustainability* 11 (19) (2019) 5492.
- [25] V.A. Parsa, E. Salehi, Spatio-temporal analysis and simulation pattern of land use/cover changes, case study: naghadeh, Iran, *Journal of Urban Management* 5 (2) (2016) 43–51.
- [26] S. Kumar, N. Radhakrishnan, S. Mathew, Land use change modelling using a Markov model and remote sensing, *Geomatics, Nat. Hazards Risk* 5 (2) (2014) 145–156.
- [27] L. Xinbin, J. Xiang, G. Nana, M. Lingran, Assessment of urban heat islands for land use based on urban planning: a case study in the main urban area of Xuzhou City, China, *Environ. Earth Sci.* 80 (8) (2021).
- [28] M.T. Sohail, Y. Mahfooz, K. Azam, Y. Yen, L. Genfu, S. Fahad, Impacts of Urbanization and Land Cover Dynamics on Underground Water in Islamabad, Pakistan, vol. 159, *Desalin Water Treat.*, 2019, pp. 402–411.
- [29] R. Zafar, S. Bashir, D. Nabi, M. Arshad, Occurrence and quantification of prevalent antibiotics in wastewater samples from Rawalpindi and Islamabad, Pakistan, *Sci. Total Environ.* 764 (2021), 142596.
- [30] A. Aslam, I.A. Rana, S.S. Bhatti, The spatiotemporal dynamics of urbanisation and local climate: a case study of Islamabad, Pakistan, *Environ. Impact Assess. Rev.* 91 (2021), 106666.
- [31] M.S. Salama, R. Van der Velde, L. Zhong, Y. Ma, M. Ofwono, Z. Su, Decadal variations of land surface temperature anomalies observed over the Tibetan Plateau by the Special Sensor Microwave Imager (SSM/I) from 1987 to 2008, *Climatic Change* 114 (3–4) (2012) 769–781.
- [32] C. Agarwal, A Review and Assessment of Land-Use Change Models: Dynamics of Space, Time, and Human Choice, *books.google.com*, 2002.
- [33] I. Maduako, Z. Yun, B. Patrick, Simulation and prediction of land surface temperature (LST) dynamics within Ikom City in Nigeria using artificial neural network (ANN), *J. Remote Sens. GIS* 5 (1) (2016) 1–7.
- [34] Z. Hassan, et al., Dynamics of land use and land cover change (LULCC) using geospatial techniques: a case study of Islamabad Pakistan, *SpringerPlus* 5 (2016) 1–11.
- [35] M.U. Saleemi, Urban change detection of Lahore (Pakistan) using the thematic mapper images of landsat since 1992–2010, in: *Proceedings of the Fourth International Conference on Aerospace Science and Engineering (ICASE 2015)*, vol. 2, 2015. Islamabad, Pakistan.
- [36] A. Raziq, A. Xu, Y. Li, Q. Zhao, Monitoring of land use/land cover changes and urban sprawl in Peshawar City in Khyber Pakhtunkhwa: an application of geoinformation techniques using of multi-temporal satellite data, *Remote Sens. GIS* 5 (4) (2016) 1–11.
- [37] Q. Weng, A remote sensing? GIS evaluation of urban expansion and its impact on surface temperature in the Zhujiang Delta, China, *Int. J. Rem. Sens.* 22 (10) (2001) 1999–2014.
- [38] A. Pandey, A. Mondal, S. Guha, P.K. Upadhyay, D. Singh, Land use status and its impact on land surface temperature in Imphal city, India, *Geology, Ecology, Landscapes* (2022) 1–15.
- [39] Q.U.Z. Chaudhry, *Climate Change Profile of Pakistan*, Asian development bank, 2017.
- [40] H. Xu, D. Lin, F. Tang, The impact of impervious surface development on land surface temperature in a subtropical city: xiamen, China, *Int. J. Climatol.* 33 (8) (2013) 1873–1883.
- [41] J.O. Adegoke, R.A. Pielke, J. Eastman, R. Mahmood, K. Hubbard, Impact of irrigation on midsummer surface fluxes and temperature under dry synoptic conditions: a regional atmospheric model study of the US High Plains, *Mon. Weather Rev.* 131 (3) (2003) 556–564.
- [42] H. Ahmad, M. Öztürk, W. Ahmad, S.M. Khan, Status of natural resources in the uplands of the Swat Valley Pakistan, *Climate change impacts on high-altitude ecosystems* (2015) 49–98.
- [43] G. Ren, et al., Urbanization effects on observed surface air temperature trends in North China, *J. Clim.* 21 (6) (2008) 1333–1348.
- [44] A. Pandey, A. Mondal, S. Guha, P.K. Upadhyay, D. Singh, A long-term analysis of the dependency of land surface temperature on land surface indexes, *Papers in Applied Geography* (2023) 1–16.
- [45] T.R. Oke, The energetic basis of the urban heat island, *Q. J. Roy. Meteorol. Soc.* 108 (455) (1982) 1–24.

- [46] S Zhang, How the Internet+ Green Public Welfare Model Cultivates a Low-Carbon and Green Lifestyle: Case of Ant Forest, *J. Urban Plan. Dev.* 149 (3) (2023), 04023015.
- [47] R.K. Pachauri, et al., *Climate Change 2014: Synthesis Report. Contribution of Working Groups I, II and III to the Fifth Assessment Report of the Intergovernmental Panel on Climate Change*, Ippc, 2014.
- [48] V. Masson-Delmotte, et al., *Climate change 2021: the physical science basis, Contribution of working group I to the sixth assessment report of the intergovernmental panel on climate change 2* (2021).